RSC Advances

PAPER

View Article Online
View Journal | View Issue



Cite this: *RSC Adv.*, 2025, **15**, 7160

# Recovering mechanoluminescence in SAOED/epoxy stress sensors with self-healing epoxy vitrimers†

Cigdem Caglayan, [a] Geonwoo Kim [a] and Gun Jin Yun *[ab]

In mechanoluminescence stress sensors, understanding the relationship between light emission performance and sensor structural stability is crucial to ensure the accuracy, sensitivity, and reliability of stress sensing during operation. Any minor structural damage or debonding at the particle–epoxy interface will reduce stress transfer capacity and hamper the light emission from SAOED particles. Instead of replacing the sensors with reduced light emission performance, self-healing epoxy vitrimers can open up new opportunities for recovering mechanoluminescence, offering durable and environmentally friendly high-performance stress sensors. This study investigates two epoxy vitrimer systems for ML stress sensors compared to commercial epoxy. Siloxane bond exchange-based ML stress sensors are found to be promising in terms of light intensity, stress sensitivity, and ML recovery. Exposing sensors to a thermal treatment revealed an increase in light intensity, which is associated with a temperature effect on SAOED particles and self-healing bond exchange in dynamic epoxy networks.

Received 20th December 2024
Accepted 9th February 2025

DOI: 10.1039/d4ra08911a

rsc.li/rsc-advances



## Introduction

Mechanoluminescence stress sensors stand out as revitalizing alternatives to traditional stress-sensing technologies. Most current research focuses on the underlying principles and intensity of light emission and the sensitivity, accuracy, and reliability of stress sensing, but it lacks sustainability considerations. Mechanoluminescence materials enable cost-effective, non-contact stress distribution detection and visualization by correlating ML intensity with the applied stress amplitude. Specifically, strontium aluminate phosphors have been broadly investigated due to their high and long-lasting light emission and fast response to mechanical actions such as tension, compression, and friction. The successful synthesis of $SrAl_2O_4:Eu^{2+}$, $Dy^{3+}$ (SAOED) particles has been reported as an alternative to ZnS:Cu phosphors, overcoming the shortcomings with brightness and afterglow durability.[1] The ML intensity in SAOED particles has been revealed to be intensely dependent on the applied stress amplitude and strain rate since the light emission is closely related to the movement of dislocations and the recombination of activated electrons and holes.[2–5] These characteristics of SAOED particles opened up excellent prospects in optomechanical devices to be used in the structural health monitoring of composites.

The effective implementation of SAOED particles has been elucidated profoundly for the sensitivity,[6–8] accuracy, and reliability[9–11] of stress sensing. In this regard, several efforts have been devoted to either synthesis methods and surface engineering of SAOED particles or the interaction of SAOED particles with the host matrix. Yet, ML stress sensor research faces challenges regarding repeatability and sustainability. For a stress sensor, the primary technical feature is to ensure outstanding performance over a prolonged time.[12,13] It can be accomplished if the structural integrity of the sensor can be preserved without any physical damage.

Until now, SAOED particles have been predominantly incorporated in commercial epoxy systems owing to their high elastic modulus and good optical transparency. Despite the significant achievements attained up to this point, utilization of commercial epoxy poses technical challenges for the further application of ML stress sensors due to their irreversible crosslinked structure. Kim *et al.*[14] confirm that SAOED/epoxy demonstrates a non-linear decrease in ultimate tensile strength and a proportional decay in ML intensity under repetitive loading. Moreover, it is noted that the reduction in light intensity is more significant and faster under increased applied stress. Even though replacing epoxy matrix with polydimethylsiloxane (PDMS) appears ideal for developing more flexible stress sensors, researchers have acknowledged a similar loss in ML performance under cyclic loading.[15–17] Besides, it is well-known that increased flexibility is likely to hamper the sensitivity of stress sensors.[12] Therefore, self-

[a]*Department of Aerospace Engineering, Seoul National University, Seoul 08826, South Korea*

[b]*Institute of Advanced Aerospace Engineering Technology, Seoul National University, Seoul 08826, South Korea. E-mail: gunjin.yun@snu.ac.kr*

† Electronic supplementary information (ESI) available. See DOI: https://doi.org/10.1039/d4ra08911a

healing ML stress sensors must be developed to repair the epoxy network's micro-level cracks without compromising sensitivity and reliability. This study explores the performance and sustainability of ML stress sensors fabricated by inserting SAOED particles in self-healing epoxy vitrimers.

Vitrimer is a crosslinked epoxy network with dynamic covalent bonds changing its topology through bond exchange reactions (BER) primarily by thermal stimulation searching for environmental-friendly epoxy system solutions.[18–20] The covalent adaptive networks (CAN) utilized in synthesizing vitrimers include but are not limited to transesterification,[21,22] imine metathesis,[23,24] disulfide,[18,25] and siloxane[19,26] exchange. With the ease of synthesis and bond exchange relatively at lower temperatures, disulfide bond exchange-based vitrimers attracted enormous research interest. In pursuit of developing dual dynamic vitrimers, Chen *et al.*[27] revealed that the activation energy required for disulfide metathesis is lower and stress relaxation is faster than carboxylate transesterification bond exchange reactions. Zhou *et al.*[28] synthesized vitrimers with double-disulfide bond exchanges and recycled ground epoxy powder in a hot press at 180 °C. Initially having an ultimate tensile strength of around 40 MPa, the double-disulfide vitrimer could recover its mechanical properties completely. In the last decade, the anionic equilibration of crosslinked siloxane bonds began to captivate a great interest after McCarthy *et al.*[29] rediscovery. The synergy of high mechanical strength from the epoxy backbone and the dynamic exchange capability of Si–O–Si bonds in the presence of a solid basic catalyst leads to the development of new high-performance self-healing epoxy composites. Debsharma *et al.*[30,31] illustrated thermoforming capacity and rapid self-healing of shear cracks in load-bearing vitrimer composites through a siloxane bond exchange mechanism. Putnam-Neeb *et al.*[26] indicated that the dynamic and mechanical performance of these epoxy vitrimers could be further tailored by altering the ratios of resin and a dynamic siloxane-containing crosslinking agent.

This study comprehensively investigates utilizing self-healing dynamic epoxy networks in ML stress sensors. The synthesis and characterization of self-healing epoxy vitrimers are initially discussed to comprehend the structural stability and self-healing mechanism's efficiency. Afterward, the sensitivity and sustainability of mechanoluminescence are examined in two different vitrimer systems consisting of aromatic disulfide metathesis and siloxane equilibration chemistry. The feasibility of employing epoxy vitrimers over commercial epoxy is discussed under single-static and repetitive loadings, comparing the formation and healing of micro-cracks morphologically and quantitatively.

## Materials and methods

### Materials

All the chemical products are commercially available and used as received without further purification. Rare-earth doped strontium aluminate (SAOED) was purchased from Nemoto & Co., Ltd., Japan. Potassium hydroxide (KOH) and deionized water are purchased from Samchun Chemicals, Korea. For the synthesis of epoxy vitrimers, diglycidyl ether of bisphenol-A (DGEBA), 2-amino-phenyl disulfide (AFD), and 3-aminopropyl diethoxymethylsilane (APEMS) are supplied from Sigma-Aldrich. Commercial epoxy resin (West System® 105 and Special Clear Hardener® 207) is used to fabricate reference samples.

### Fabrication of self-healing ML epoxy vitrimers

Self-healing ML stress sensors are prepared by dispersing SAOED particles in DGEBA resin. For the fabrication of self-healing ML stress sensors with aromatic disulfide BER (ML/VT), SAOED/DGEBA mixture is mixed with 2-AFD with a resin-to-hardener molar ratio of 3 : 2 and stirred at 80 °C for 40 min. The mixture is degassed at 80 °C for one hour and cured at 120 °C for 12 h.

In the case of dynamic siloxane BER-based self-healing ML stress sensors (ML/SVT), the hardener (K-PAMS) is synthesized in the laboratory based on previously reported literature studies.[19,26,32] APEMS is chosen as the starting material, and KOH is introduced as a catalyst to generate catalytic potassium silanolate end groups on the hardener backbone. The detailed synthesis method can be found in Fig. S1.† SAOED/DGEBA is mixed with K-PAMS in equivalent weight and stirred gently for 5 min at 50 °C. The mixture is degassed at 50 °C for 20 min and then taken into preheated silicon molds to be cured at 80 °C for 24 h.

Reference ML stress sensors (ML/Ep) are fabricated by directly mixing West System® resin and hardener in a weight ratio of 100 : 33. The samples are degassed at RT and cured at 80 °C for 12 h (Table 1).

### Characterization

To decide a proper self-healing process temperature that enables adequate chain mobility and bond exchange reactions to take place, the glass transition temperatures are analyzed by differential scanning calorimetry (DSC) at a heating rate of 10 °C $min^{-1}$ from 40 °C to 200 °C using Discovery (TA Instruments). Thermal gravimetric analysis (TGA) are carried out from 30 °C to 800 °C under nitrogen atmosphere at a heating rate of 10 °C $min^{-1}$. The stress relaxation behavior of vitrimers is validated by analyzing by DMA/Q800, TA Instruments. The samples are subjected to a strain of 1% in the linear region at 150 °C for Ep and VT and at 120 °C for SVT. The stress relaxation responses are monitored for one hour to confirm the presence of chain motion and bond exchange. The curing state of vitrimers is confirmed by FTIR (Thermo Scientific Nicolet 6700) to ensure any change in mechanical performance after the self-healing procedure is not related to a post-curing. The morphological characterization of ML stress sensors is investigated by scanning electron microscopy (SEM) and X-ray microscopy (XRM). For SEM analysis, the samples are microtome-machined into 500 nm thick slices using a diamond blade. Due to the brittle nature of SAOED particles, some larger particles on the surface were shredded during the microtome process. In this study, SEM analysis is primarily focusing on the interface between epoxy and particles underneath after testing and self-healing procedures.

Table 1 Compositions of synthesized ML stress sensors

| Sample | SAOED weight fraction (wt%) | Bond exchange reaction mechanism (BER) |
|---|---|---|
| ML/Ep | 10 | — |
| | 20 | |
| ML/VT | 10 | Aromatic disulfides |
| | 20 | |
| ML/SVT | 10 | Potassium silanolates |
| | 20 | |

### Self-healing and ML performance evaluation of epoxy vitrimers

The mechanoluminescence characteristics of ML stress sensors are investigated under uniaxial tensile testing using the Psylotech MicroTs testing machine. A strain of up to 2.5% with a testing speed of 100 μm $s^{-1}$ is applied repetitively. The tests are conducted in a completely dark environment where the samples are UV-irradiated for 5 min and left for stress-free decay for 5 min. The ML response of samples is recorded simultaneously by a Grasshopper 3 (FLIR Systems) camera connected to PTGrey Fly Capture 2 software. A picture is taken every five μm of displacement increment. Recorded images are converted to binary images from a gray-scale version using MATLAB®. The magnitude of ML intensity is calculated in two steps as given by;

$$\mathrm{LI} = \mathrm{PIV}_{\mathrm{gauge}} - \mathrm{PIV}_{\mathrm{edge}} \text{ in a single image} \quad (1)$$

and

$$\mathrm{LIC}^i = \mathrm{LI}^i - \mathrm{LI}^0 \text{ for } i = 0, 1, 2, 3, \ldots, n \quad (2)$$

in which $n$ is the total number of images. At first, the light intensity (LI) for each image is evaluated by subtracting pixel intensity values of the far-field background region ($\mathrm{PIV}_{\mathrm{edge}}$) from the reference gauge area ($\mathrm{PIV}_{\mathrm{gauge}}$), eqn (1). Then, the mechanoluminescence light intensity changes at a given time ($\mathrm{LIC}^i$) is defined as the difference of PIV between the current image ($\mathrm{LI}^i$) and the initial image ($\mathrm{LI}^0$) at $t = 0$, eqn (2).

Besides, straightforward image processing is performed by clustering the light intensity variation throughout the sample based on the changes in pixel intensity. This approach allows the light intensity change in the sample to be visualized easily and quickly under applied loading. A schematic drawing of the experimental set-up is depicted in Fig. 3a.

In the case of self-healing, ML stress sensors are thermally treated at 100 °C for 5 hours in a convection oven after 30 cycles to trigger bond exchange and repair potential micro-level cracks and voids around SAOED particles. After cooling down, the samples are kept at room temperature overnight. Then, the same loading conditions are applied, including UV-excitation before testing again. The exact loading and thermal-treatment

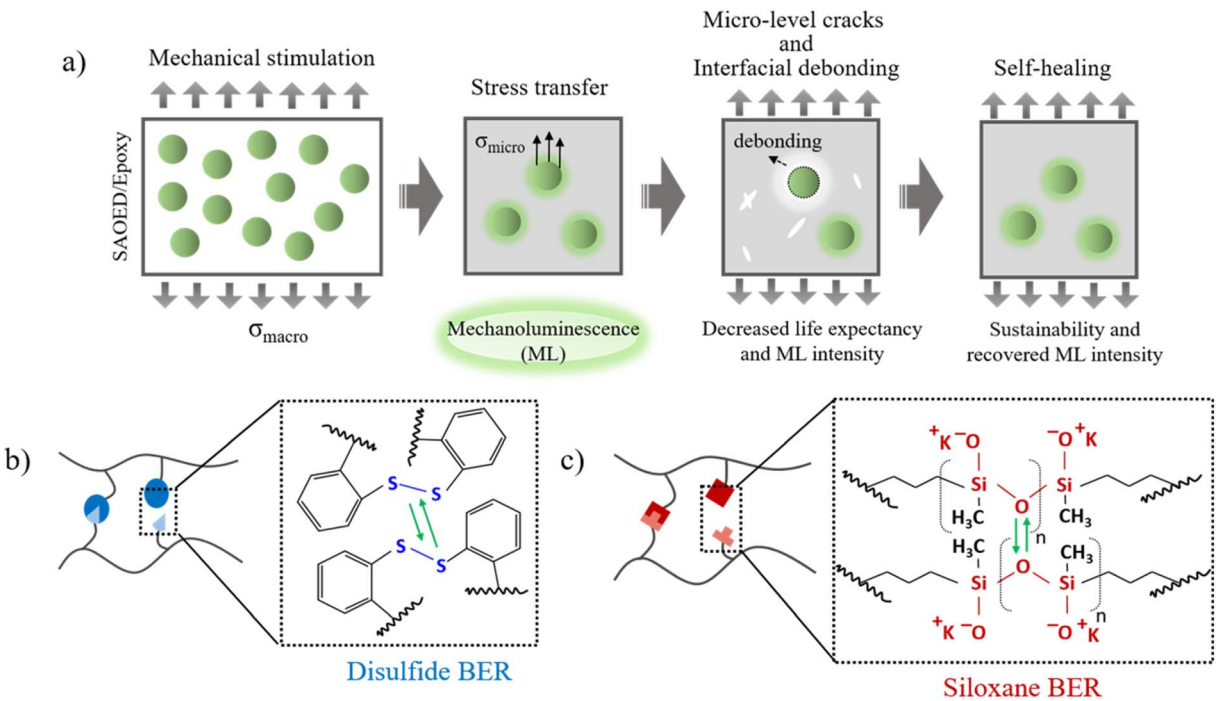


Fig. 1 (a) Schematic diagram of potential micro-level cracks, particle–epoxy interfacial debonding, and self-healing mechanism for the recovery of ML intensity (b) aromatic disulfide BER and (c) dynamic siloxane BER-based epoxy vitrimers.

procedures are repeated for reference epoxy networks for comparison. Herein, it should be noted that performing the same thermal procedure on ML/VT, ML/SVT, and ML/Ep sensors helps to avoid the temperature effect on SAOED light emission, which is out of the scope of this study.

## Results and discussion

### Material design and characterization

The present study compares ML stress sensors utilizing three epoxy systems, including commercial epoxy and vitrimers (Fig. 1). Through a systematic analysis, these materials' chemical, thermal, and mechanical properties are elucidated to determine the most suitable polymer matrix and working conditions for the sustainability of sensors. Epoxy vitrimer systems are constructed with covalent adaptive networks by introducing aromatic disulfides and catalytic potassium silanolates. FTIR investigates the curing states of VT and SVT networks to confirm the success of synthesis, as shown in Fig. 2a. The characteristic epoxide group peak at 914 $cm^{-1}$ disappears in both vitrimers, indicating complete reaction conversion after curing. The dominant peak of Si–O–Si stretching vibration remains detectable approximately at 1060 $cm^{-1}$ in SVT.

Fig. 2b illustrates the glass transition temperatures ($T_g$) determined based on the inflection point of the sigmoid $T_g$ transition. The results indicate that VT shows a moderately higher $T_g$ than Ep. It is likely ascribed to its higher crosslink density, as evidenced by its superior mechanical strength. SVT displays the lowest $T_g$ among all systems due to Si–O bonds, which allow more chain rotation and mobility.[33]

Since the motivation of this study is to investigate the role of self-healing vitrimers in ML stress sensors, stress relaxation tests are conducted to systematically compare the bond exchange activity of these two vitrimers. In contrast to commercial epoxy, reversibly driven by aromatic disulfide and siloxane bond exchange reactions, VT and SVT endow a complete stress relaxation at 150 and 120 °C, respectively. The dynamic Si–O–Si bond shows a faster relaxation behavior than S–S bonds, even at a lower temperature. Considering the recovery of the original mechanical strength, Fig. 2c indicates that SVT promises a higher chance of self-healing, recovered stress transfer, and light emission correlatively.

Besides, an approximate comparison of vitrimer bond exchange efficiency is performed by tensile tests before and after reshaping the synthesized vitrimers to address the self-healing bond exchange efficiency in ML stress sensors. Initially, the original samples are tested under a tension load until fracture. Fig. 2d depicts an ultimate strength of 80 (±1.6) and 90 (±3.3) MPa for commercial epoxy and VT, respectively. Meanwhile, SVT owns a strength of 55 (±1.3) MPa. Despite the observed decrease in the ultimate tensile strength, SVT offers a better strain at break (11–12%) due to the flexibility and chain mobility of siloxane backbones. Fig. 2e displays pellets formed

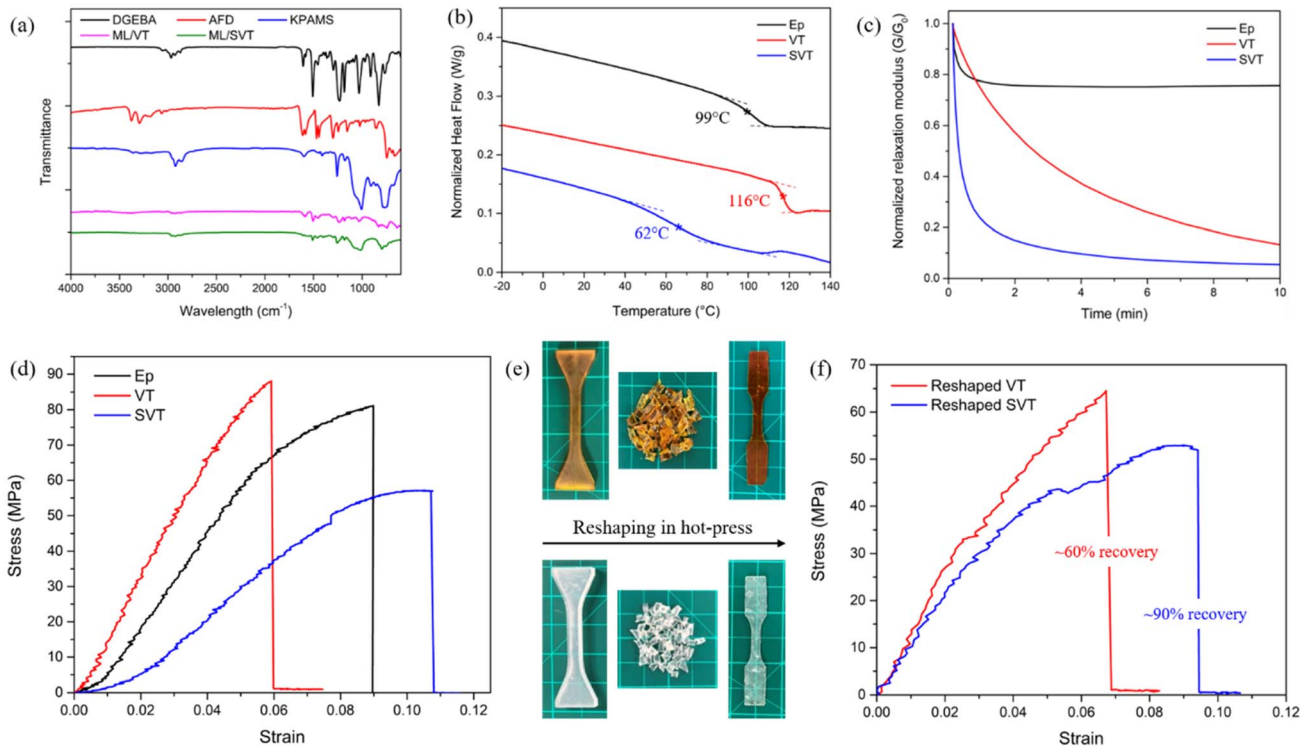


Fig. 2 Characterization of epoxy vitrimers and evaluation of reshaping capacities through BER (a) FTIR spectrum of epoxy precursors and synthesized ML vitrimers (b) DSC analysis to determine $T_g$ of commercial and synthesized epoxy networks (c) stress relaxation behavior of all networks to demonstrate the potential of self-healing ability (d) tensile strength of neat epoxy networks (e) reshaping VT by hot-pressing at 180 °C, and SVT at 120 °C for 6 hours (f) recovery of tensile strength after reshaping process.

from these vitrimers after the tension test and their reshaping to 2nd generation vitrimers in the form of tensile coupons. Reshaping is performed by hot-pressing at 180 °C and 120 °C for VT and SVT samples for 6 hours, respectively. The reshaping and self-healing temperatures in this study are selected to be moderately above $T_g$ and below $T_d{}^{5\%}$ ensuring that bond exchange reactions occur efficiently without degradation. The efficiency of reshaping ($\delta_{reshaping}$) the epoxy vitrimers is calculated following eqn (3);

$$\delta_{reshaping}\ (\%) = [\sigma_{reshaped}/\sigma_{original}] \times 100\% \quad (3)$$

where $\sigma_{original}$ is the ultimate tensile strength of the original sample and $\sigma_{reshaped}$ is the ultimate tensile strength of reshaped sample. Fig. 2f proves the superior network stability of reshaped SVT as evidenced by the full recovery of ultimate tensile strength and strain at break. On the other hand, VT demonstrates a relatively poor performance than SVT by recovering approximately 60% of the original tensile strength.

As a result, it is deduced that epoxy vitrimers with dynamic siloxane bonds outperform aromatic disulfides in terms of chain mobility and efficiency of bond exchange reactions. SVT requires a lower process temperature for reshaping than VT and yields a nearly perfect recovery of mechanical properties. In this scope, SVT is foreseen as the more appropriate candidate for use in ML stress sensors, considering its potential in self-healing minor-level cracks and interfacial debonding.

### Comparison of ML stress sensing in different epoxy networks

ML stress sensors are subjected to single static tension tests with a strain rate of 100 μm $s^{-1}$ to determine the optimal SAOED amount. Before studying the self-healing ability of ML stress sensors, the amount of SAOED inclusion is decided for all epoxy systems to ensure the accuracy of light emission comparison.

Fig. 3 illustrates the light intensity change in different polymer matrices despite the same amount of SAOED particles. Under the same loading conditions, 10-ML/Ep shows the highest light emission, followed by 10-ML/SVT as the second highest. The lower light intensity in 10-ML/SVT is associated with its relatively higher flexibility at the break. The light emission of 10-ML/VT is significantly lower and almost

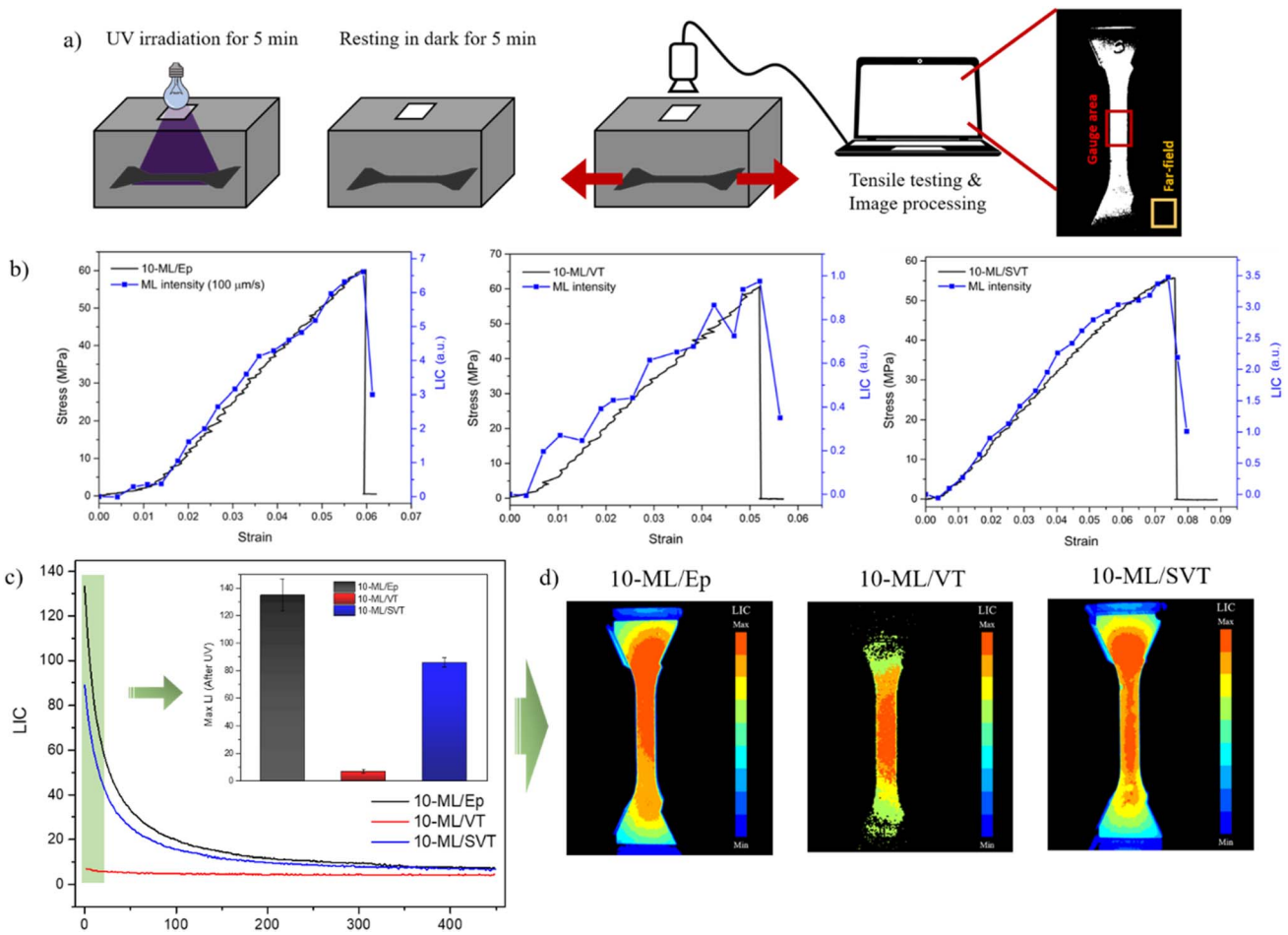


Fig. 3 (a) Schematic overview of ML intensity test set-up in dark environment (b) light intensity change (LIC) of ML-epoxy sensors under single static loading with a strain rate of 100 μm $s^{-1}$ (c) afterglow intensity change of commercial epoxy and epoxy vitrimers under same excitation conditions (inset: maximum light intensity after 5 minutes of UV-excitation) (d) visualization of maximum light intensity variation in ML/Ep, ML/VT and ML/SVT after UV excitation.

ignorable compared to the stress-light intensity-strain graphs in Fig. 3. The immense disparity in the light emission characteristics of ML/VT and ML/SVT implies the importance of the opacity of the chosen polymer matrix.

The optical transparency of the selected matrix is crucial to avoid blocking the stress-induced light emission.[12,34,35] Therefore, photoluminescence and the stress-free afterglow behavior of commercial epoxy and epoxy vitrimers with 10 wt% SAOED are compared after 5 min of UV irradiation based on the images recorded by the digital camera. ML/Ep and ML/SVT demonstrate a bright light emission that the naked eye can observe. Keeping the sample stress-free for 7 minutes, a rapid decay in light intensity with an afterglow of around 3 minutes is present in both samples. The sharp decrease in light intensity and afterglow in SAOED particles are associated with the intrinsic lifetime of $Eu^{2+}$ and thermal trapping–detrapping of charge carriers,[36] respectively. In the meantime, ML/VT does not demonstrate a remarkable light emission or an afterglow due to the natural dark yellowish color of disulfide-bonded epoxy network, as seen in Fig. 2e. Once more, Fig. 3c implies the importance of matrix selection in terms of transparency, considering the maximum light intensities. Consequently, the amount of SAOED inclusion is determined to be doubled for all samples to facilitate the quantification of ML intensity more clearly.

When the weight fraction of SAOED particles is increased to 20%, the light intensity in ML/VT is noticed to be 200% higher than that for 10-ML/VT, Fig. 4. It reveals that the light permeation deficiency related to the opacity in disulfide-bonded epoxy networks can be overcome by embedding more SAOED particles. Yet, this might raise another challenge of homogeneous SAOED dispersion in epoxy. Moreover, Fig. 4 reveals that the light intensity of 20-ML/VT is still remarkably lower than 20-ML/Ep and 20-ML/SVT. The inadequate light emission in ML/VT limits their utility in stress sensing for the time being. Hence, ML/VT is eliminated from further investigation at this stage and is not subjected to cyclic loading. The photoluminescence intensity and light transmittance of 20-ML/Ep and 20-ML/SVT are investigated thoroughly by photoluminescence spectrometer and UV/vis spectrophotometer. Fig. S4 and Table S3† reveal that 20-ML/Ep exhibits higher PL intensity and lower transmittance compared to 20-ML/SVT, likely due to the structural differences in their crosslinked networks.

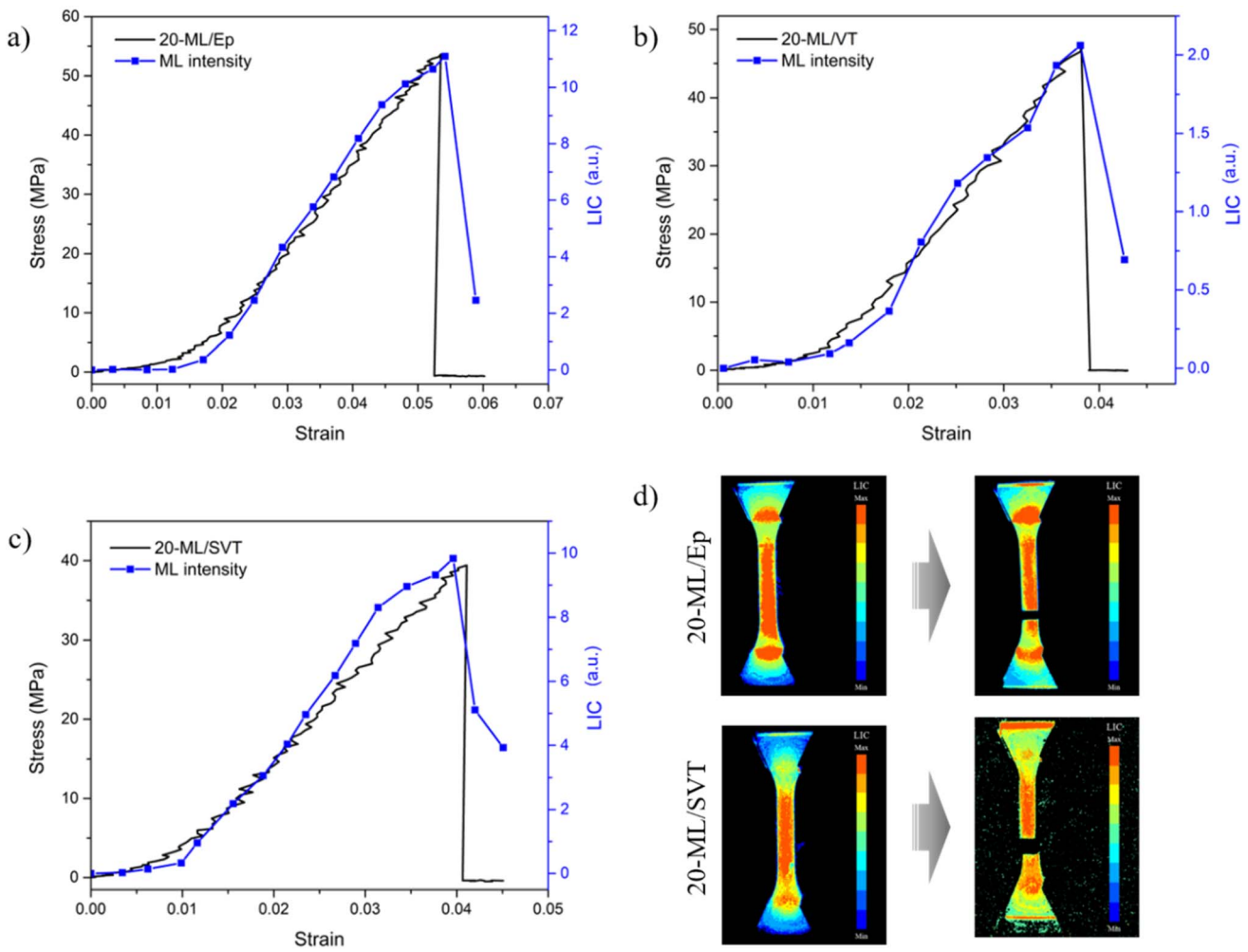


Fig. 4 ML intensity of (a) ML/EP, (b) ML/VT and (c) ML/SVT under single static loading with a strain rate of 100 μm $s^{-1}$ (d) binarized and colorized images of ML-epoxy samples before and after fracture.

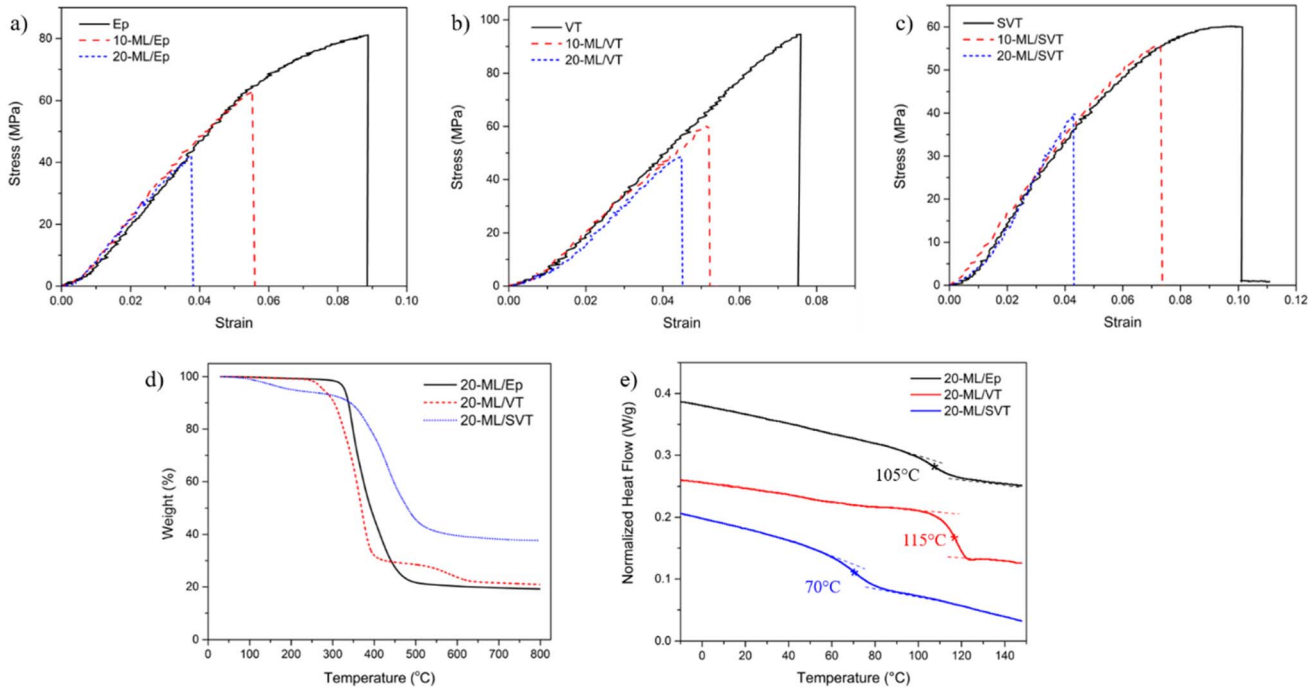


Fig. 5 (a–c) Tensile strength of ML stress sensors with varying SAOED concentration (d) thermal stability and (e) glass transition temperatures of ML stress sensors.

By doubling SAOED concentration, the mechanoluminescence light intensity is increased by around 65% and 180% in ML/Ep and ML/SVT, respectively. The extreme change in ML/SVT light emission is associated with increased brittleness, which makes it more sensitive to the applied stress. Fig. 4 illustrates that when the amount of SAOED is increased, the light emission in 20-ML/SVT becomes comparable to 20-ML/Ep. It promises the potential of dynamic siloxane BER-based epoxy vitrimers as a viable alternative to commercial epoxy.

Fig. 5 illustrates the variation in the mechanical performance of ML stress sensors under tensile loading, evaluated at different weight fractions of SAOED. Increasing the SAOED concentration leads to a reduction in the ultimate tensile strength across all epoxy networks. Similarly, the strain at break exhibits a corresponding decrease, whereas the stiffness remains nearly constant, as given in Table S1.† The tensile test results highlight the necessity to control the SAOED concentration to achieve an optimal trade-off between the light emission and mechanical performance. Due to the brittle nature of SAOED particles, higher concentrations might compromise the flexibility of stress sensors.[15,37] The synergistic interaction between SAOED and epoxy, and the quality of SAOED dispersion and distribution can be considered as another key factors determining the mechanical performance. Fig. S3† displays the morphology of 20-ML/SVT surface trimmed using a microtome diamond blade, representatively. SAOED particles are observed to distribute uniformly within the polymer matrix, taking particle size and shape variation into account. Yet, the weak interaction between SAOED particles and epoxy reduces stress transfer gradually. These aspects are elucidated thoroughly in the following section connecting them to the overall ML performance.

Comparing the thermal stability of ML stress sensors, 20-ML/Ep exhibits the best performance with a thermal decomposition temperature of 329 °C at 5% weight loss, Table S2.† Meanwhile, 20-ML/SVT exhibits an earlier onset of decomposition, with a 5% weight loss observed at 204 °C. The chain scission of C–O bonds and breakdown of crosslinked networks in epoxy is responsible for the initial degradation of epoxy networks.[38,39] Since the siloxane backbones contribute to a lower crosslink density and lower stiffness, the degradation starts earlier and there is a decrease in the onset decomposition temperature in 20-ML/SVT.[26,33,40] Contrarily, the decomposition temperature at 50% weight loss is higher for 20-ML/SVT which is associated with higher energy required for Si–O bond scission.[41] The final residue in 20-ML/Ep and 20-ML/VT around 20% reveals the SAOED concentration. In 20-ML/SVT, the final residue, which is approximately 40%, is assumed to contain silicon in addition to SAOED particles. Additionally, DSC scans of ML stress sensors show no significant change in glass transition temperatures relatively to neat epoxy networks previously discussed.

## Self-healing and recovery of ML intensity

The repeatability of ML response is essential to maintain the same transduction ability for long-term stress sensing applications with high reliability.[42] The sustainability of light emission in mechanoluminescence epoxy networks is characterized under repetitive loading–deloading conditions based on strain-controlled tensile testing. The ML intensity is superimposed on

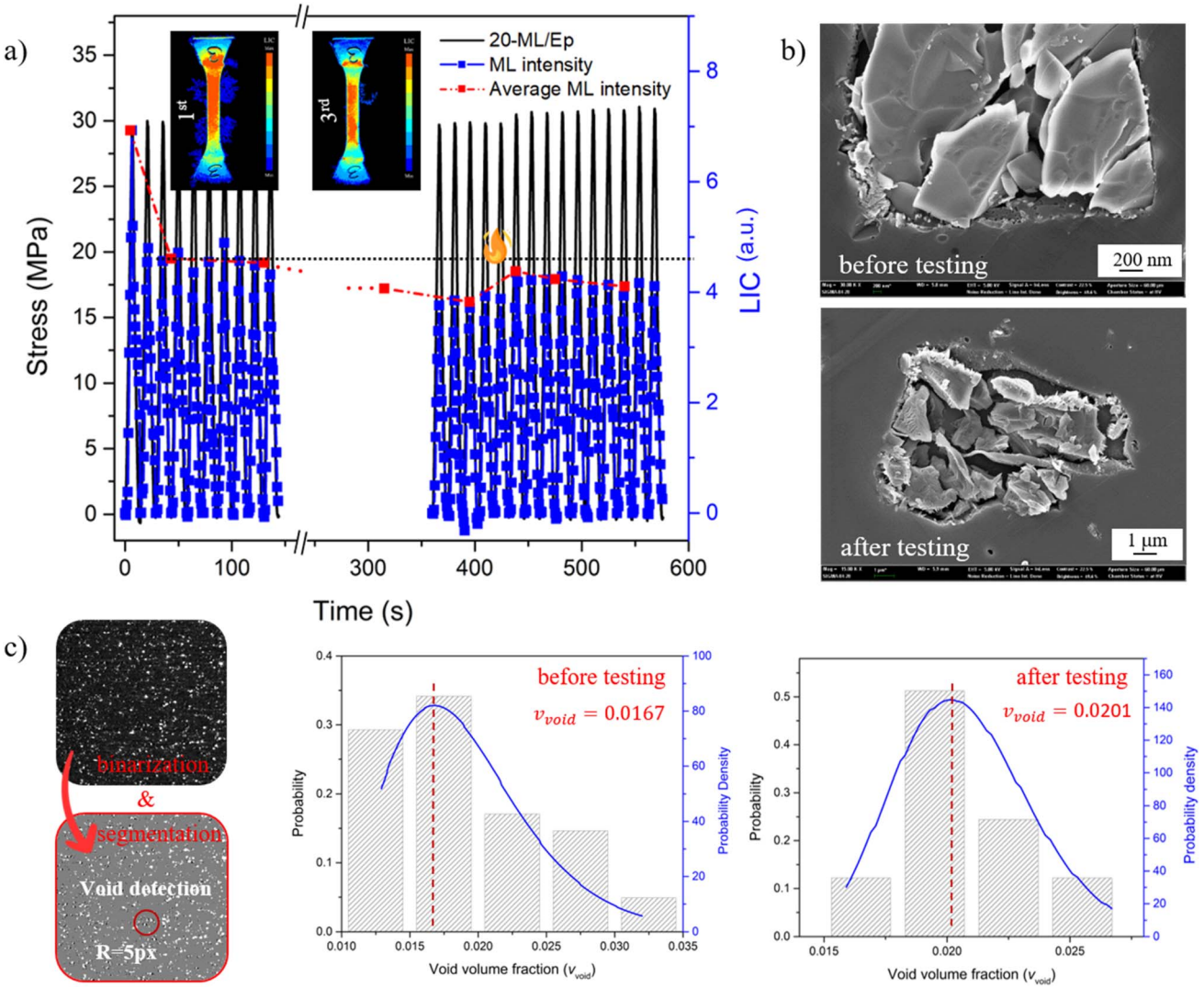


Fig. 6 (a) Gradual decrease in light intensity commercial epoxy-based ML stress sensors under cyclic testing (b) SEM images of the clean-cut surfaces of ML/Ep stress sensor before tensile testing, after 30 times cyclic testing (c) the estimated void fractions before and after cyclic testing based on XRM image processing results.

the applied loading cycle concerning the time-lapse as illustrated in Fig. 6a. Fig. 6a shows the response of 20-ML/Ep under repetitive tensile loading with UV excitation applied before each loading cycle. Despite the periodic reaction during the entire loading cycle, the light intensity is inconsistent with the amplitude of applied load after the first loading. The light intensity drops more than 30% after the first loading cycle, during which the sample is stretched up to a strain of 2.5% for the first time. It should be noted that a strain of 2.5% corresponds to a stress amplitude of 55% for 20-ML/Ep. Therefore, the detected decay in light intensity during the first stretching can be associated with the initial energy release within microstructural adjustments. Afterwards, the decay continues around 10% more over time regardless of UV-excitation state, *etc.* This gradual decrease is ascribed to generating micro-level voids and breaking down some crosslinks. After testing 30 times, the total loss of ML intensity is evaluated at around 44%, implying the importance of light emission fatigue in ML stress sensors.

To understand the reason behind such a loss in ML performance, SEM analysis is conducted before and after tensile testing. Initially, in Fig. 6b, the interaction of SAOED and epoxy seems moderate, considering no additional efforts have been performed to functionalize the particles or no further mechanical procedures, such as ultrasound sonication, were taken. Yet, after 30 times of cyclic tensile testing, SAOED particles are identified to be detached from the epoxy matrix in some regions. The debonding at particle–polymer interfaces occurs in many cases when the applied macro-stress exceeds the interfacial strength of the composite.[43] Hence, tracking the void formation, especially around particles, is critical to properly understanding stress transfer and ML performance. The same samples are scanned with XRM to estimate void formation, as shown in Fig. 6c briefly. The detailed evaluation method for void formation around SAOED particles is described in Fig. S5.† The void fraction in 20-ML/Ep after 30 times of tensile testing is detected to be increasing by approximately 21%, Table 2. This

Table 2 Light intensity and void fraction change of ML stress sensors before, after testing and self-healing procedure

| | Light intensity change (LIC) | | | Void fraction | |
|---|---|---|---|---|---|
| Commercial *vs.* self-healing ML stress sensors | After 1st test | Between 2nd and 30th | After SH procedure | After testing | After SH procedure |
| 20-ML/Ep | −33.7% | −15.5% | +12.9% | +21% | — |
| 20-ML/SVT | −37.7% | −16.6% | +33.7% | +25% | −8% |
| Ref-ML/SVT[a] | −27.4% | −12.9% | +20.8% | — | — |

[a] Ref-ML/SVT represents reference 20-ML/SVT sample produced with PAMS only which does not contain potassium silanolate end groups.

result and a decrease in ML intensity support the assumption of the relation between void formation, loosened interfacial bonding and mechanoluminescence performance.

A similar trend in ML intensity change is noticed in ML/SVT after the first-time testing, Fig. 7. Repeating the tensile test 30 times, a similar total loss of 48% in light emission is recorded. After 30 times of testing, it was decided to leverage the self-healing ability of SVT vitrimer to reverse the decreasing trend in light intensity. For this reason, the 20-ML/SVT sample is kept at 100 °C for five hours and left resting at RT for one night. When tested under the same conditions, the ML intensity increases by approximately 33% compared to the previous before self-healing. Such a recovery can be mainly associated with three parameters: self-healing of voids, post-curing effect, or temperature effect on SAOED particles. To explicitly investigate which of these factors plays a more significant role in light emission recovery, XRM, FTIR, and control samples were studied comparatively. First, the void fraction estimation based on XRM images is performed identically to 20-ML/Ep, Fig. 7b. According to XRM analysis, the void fraction is estimated to increase by around 25% after 30 times of testing. Fig. 7c also confirms that the interfacial bonding between SAOED and SVT

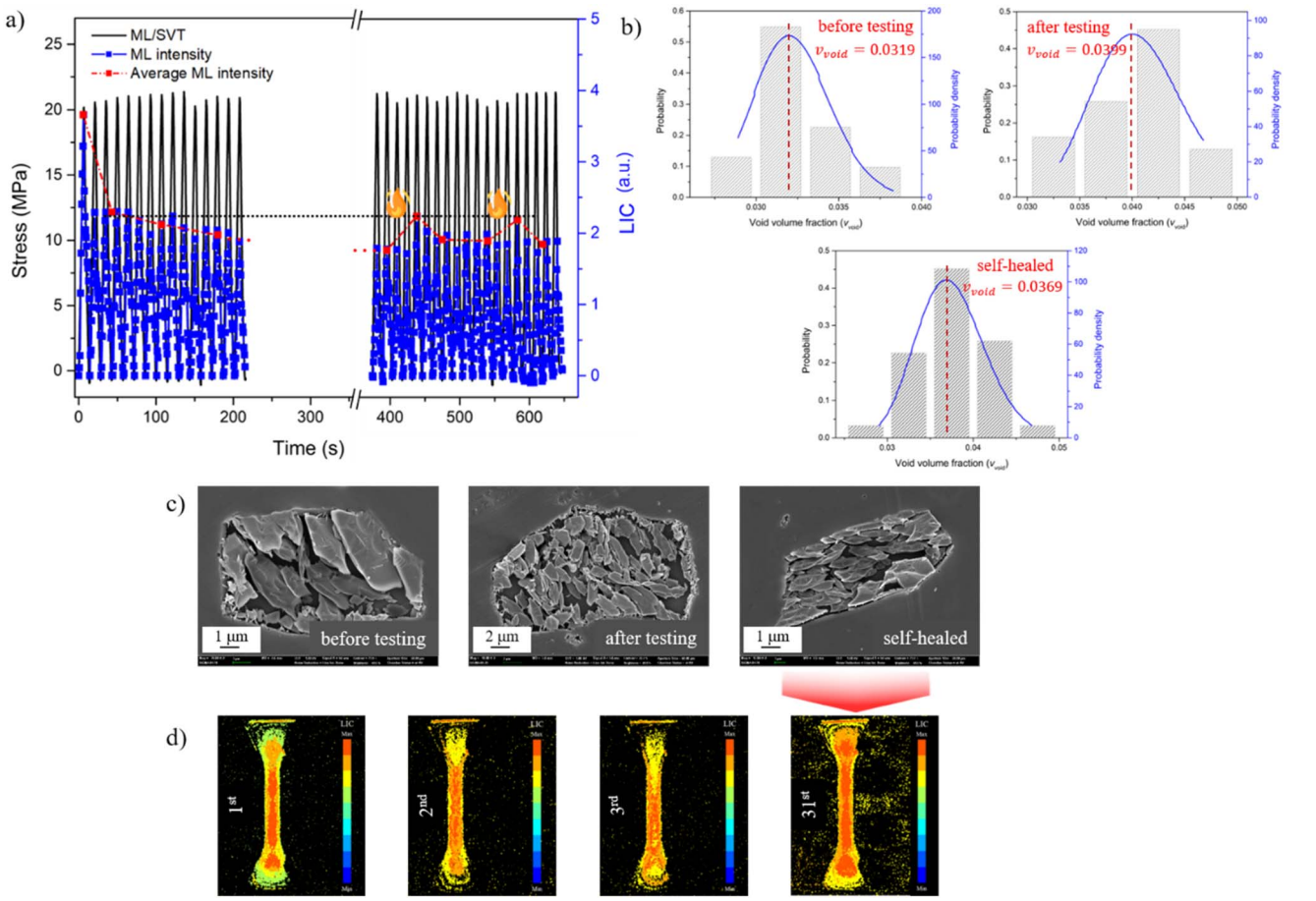


Fig. 7 (a) Stress sensing performance of ML/SVT under cyclic testing (b) the estimated void fractions before, after cyclic testing and after self-healing treatment (c) SEM images of the clean-cut surfaces of ML/SVT stress sensor before tensile testing, after 30 times cyclic testing up to a strain of 2.5% and self-healing process (d) visualized images of ML/SVT during tests demonstrating the changes in light emission step by step.

begins to loosen after 30 times tensile testing. Meanwhile, the thermal procedure applied for self-healing seems to be recovering around 8% of generated voids around SAOED particles, Table 2, implying the role of siloxane bond-exchange reactions. To distinguish this recovery from the siloxane backbone relaxation effect, 20-ML/SVT can be compared with a control sample, Ref-ML/SVT, in which there are no potassium silanolate end groups. Ref-ML/SVT shows only about 20% recovery in light emission after the same thermal procedure. Considering the siloxane chain relaxation exists in both samples, the difference in light emission recovery between 20-ML/SVT and Ref-ML/SVT is attributed to the additional bond exchange reactions in 20-ML/SVT, which accelerate both the relaxation process and healing of generated voids. Even though it is not a full recovery of voids, there is a moderate enhancement in light intensity and performance of the ML stress sensor. To verify that this enhancement is not related to a post-curing effect, FTIR peak analysis is performed for as-produced and self-healed samples, Fig. S6.† Given that the curing degree of as-produced 20-ML/SVT is already around 95%, Table S4† shows that the recovery of voids and micro-cracks is due to siloxane bond exchange reactions and not connected with additional cross-linking.

Moreover, to clarify that the light emission recovery in 20-ML/SVT is not significantly associated with a temperature effect, the same procedure is applied to 20-ML/Ep. The effect of temperature on photoluminescence and mechanoluminescence of non-piezoelectric crystals is a well-known fact, yet still not fully elucidated. The photoluminescence of SAOED particles is reported to be decreasing with an increase in temperature due to thermal quenching of luminescence.[44] At the same time, mechanoluminescence is noted to increase with temperatures up to 200 °C in oxidizing atmosphere (air) through $Eu^{2+} \Leftrightarrow Eu^{3+}$ redox reactions and movement of dislocations.[45] The light emission in 20-ML/Ep is restored by around 13% after performing the same thermal procedure. It should be pointed out that the enhancement of light emission intensity in 20-ML/Ep is less than 20-ML/SVT. It clarifies that the enhancement in ML/SVT can be ascribed to the temperature effect and the ease of chain rearrangement within catalytic potassium silanolate end groups.

Even though self-healing epoxy vitrimers are promising to replace their commercial counterparts in ML stress sensor applications, maintaining the stress transfer at the particle–epoxy interface is the most critical step for performance sustainability. This study shows that self-healing dynamic epoxy networks are advantageous yet cannot fully heal voids generated around particles after cyclic loading. Therefore, the effect of the self-healing process is a short-lived enhancement in light emission. To achieve a more durable self-healing effect, additional self-healing bond exchange reactions directly on the surface of SAOED particles might be another effective strategy for future work.

## Conclusions

This paper enlightens the potential use of self-healing epoxy vitrimers in ML stress sensors compared to commercial epoxy. The motivation behind self-healing epoxy vitrimers is to repair minor cracks and voids generated during the operation lifetime of the stress sensors, affecting the overall light emission performance. Among two different vitrimer systems, disulfide bond exchange-based ML stress sensors (ML/VT) are eliminated due to their natural yellowish color blocking the light emission. Cyclic testing is performed only for siloxane bond exchange-based ML stress sensors (ML/SVT) and for commercial epoxy as a reference. It is proven that ML stress sensors exhibit a gradual decrease of around 45% under cyclic loading of 30 times up to a strain of 2.5%. Applying a thermal treatment at 100 °C for five hours to both samples, the light intensity is increasing 13% and 33% for 20-ML/Ep and 20-ML/SVT, respectively. Ignoring the temperature effect, 20-ML/SVT still shows a higher degree of enhancement in light emission, ascribed to the ease of chain mobility *via* catalytic potassium silanolates. Yet, the light emission drops shortly after the self-healing procedure, implying the importance of self-healing through the structure and at the particle–epoxy interface.

Until now, the main focus of SAOED/epoxy stress sensor research was on improving brightness, sensitivity, interfacial bonding, *etc.* The findings of this study can contribute to further research on enhancing the self-healing efficiency in ML stress sensors to ensure a durable performance regardless of any structural damage.

## Data availability

The data that support the findings of this study are available from the corresponding author upon reasonable request.

## Conflicts of interest

The authors declare no conflicts of interest.

## Acknowledgements

This work was supported by the Institute of Engineering Research at Seoul National University. The authors are grateful for their support. This material is also based upon work supported by the Air Force Office of Scientific Research under award number FA2386-20-1-4067. This work was also supported by the BK21 Program funded by the Ministry of Education (MOE, Korea) and the National Research Foundation of Korea (NRF-4199990513944). The authors are grateful for their support. We also thank the Research Institute of Advanced Materials and National Instrumentation Center for Environmental Management for conducting part of the analysis.

## References

1 T. Matsuzawa, Y. Aoki, N. Takeuchi and Y. Murayama, A new long phosphorescent phosphor with high brightness SAOED, *J. Electrochem. Soc.*, 1996, **143**(8), 2670–2673.
2 M. Akiyama, C.-n. Xu, K. Nonaka and T. Watanabe, Intense visible light emission from $Sr_3Al_2O_6$:Eu,Dy, *Appl. Phys. Lett.*, 1998, **73**(21), 3046–3048.

3 C.-N. Xu, X.-G. Zheng, M. Akiyama, K. Nonaka and T. Watanabe, Dynamic visualization of stress distribution by mechanoluminescence image, *Appl. Phys. Lett.*, 2000, **76**(2), 179–181.
4 M. Akiyama, C.-N. Xu, Y. Liu, K. Nonaka and T. Watanabe, Influence of eu,dy co-doped strontium aluminate composition on mechanoluminescence intensity, *J. Lumin.*, 2002, **97**, 13–18.
5 G. J. Yun, M. R. Rahimi, A. H. Gandomi, G.-C. Lim and J.-S. Choi, Stress sensing performance using mechanoluminescence of SrAl2O4:Eu (SAOE) and SrAl2O4:Eu, Dy (SAOED) under mechanical loadings, *Smart Mater. Struct.*, 2013, **22**(5), 055006.
6 Y. Fujio, C.-N. Xu, M. Nishibori, Y. Teraoka, K. Kamitani, N. Terasaki and N. Ueno, Development of highly sensitive mechanoluminescent sensor aiming at small strain measurement, *J. Adv. Dielectr.*, 2014, **4**(2), 1450016.
7 T. W. Kerekes, H. You, T. Hemmatian, J. Kim and G. J. Yun, Enhancement of mechanoluminescence sensitivity of SrAl2O4: Eu2+, Dy3+/epoxy composites by ultrasonic curing treatment method, *Compos. Interfaces*, 2020, **28**(1), 77–99.
8 H. Song, S. Timilsina, J. Jung, T. S. Kim and S. Ryu, Improving the Sensitivity of the Mechanoluminescence Composite through Functionalization for Structural Health Monitoring, *ACS Appl. Mater. Interfaces*, 2022, **14**(26), 30205–30215.
9 K. S. Sohn, M. Y. Cho, M. Kim and J. S. Kim, A smart load-sensing system using standardized mechano-luminescence measurement, *Opt. Express*, 2015, **23**(5), 6073–6082.
10 H. G. Shin, S. Timilsina, K. S. Sohn and J. S. Kim, Digital Image Correlation Compatible Mechanoluminescent Skin for Structural Health Monitoring, *Adv. Sci.*, 2022, **9**(11), e2105889.
11 S. Y. Ahn, S. Timilsina, H. G. Shin, J. H. Lee, S. H. Kim, K. S. Sohn, Y. N. Kwon, K. H. Lee and J. S. Kim, In situ health monitoring of multiscale structures and its instantaneous verification using mechanoluminescence and dual machine learning, *iScience*, 2023, **26**(1), 105758.
12 Y. Zhuang and R. J. Xie, Mechanoluminescence Rebrightening the Prospects of Stress Sensing: A Review, *Adv. Mater.*, 2021, **33**(50), e2005925.
13 J. Yang, Z. Zhang, Y. Yan, S. Liu, Z. Li, Y. Wang and H. Li, Highly Stretchable and Fast Self-Healing Luminescent Materials, *ACS Appl. Mater. Interfaces*, 2020, **12**(11), 13239–13247.
14 S. Timilsina, R. Bashnet, S. H. Kim, K. H. Lee and J. S. Kim, A life-time reproducible mechano-luminescent paint for the visualization of crack propagation mechanisms in concrete structures, *Int. J. Fatig.*, 2017, **101**, 75–79.
15 P. Jha and A. Khare, SrAl2O4:Eu,Dy mechanoluminescent flexible film for impact sensors, *J. Alloys Compd.*, 2020, **847**, 156428.
16 V. K. Chandra, B. P. Chandra and P. Jha, Self-recovery of mechanoluminescence in ZnS:Cu and ZnS:Mn phosphors by trapping of drifting charge carriers, *Appl. Phys. Lett.*, 2013, **103**(16), 161113.
17 P. Zhang, J. Wu, L. Zhao, Z. Guo, H. Tang, Z. Wang, Z. Liu, W. Chen and X. Xu, Environmentally Stable and Self-Recovery Flexible Composite Mechanical Sensor Based on Mechanoluminescence, *ACS Sustain. Chem. Eng.*, 2023, **11**(10), 4073–4081.
18 A. R. d. Luzuriaga, R. Martin, N. Markaide, A. Rekondo, G. Cabañero, J. Rodríguez and I. Odriozola, Epoxy resin with exchangeable disulfide crosslinks to obtain reprocessable, repairable and recyclable fiber-reinforced thermoset composites, *Mater. Horiz.*, 2016, **3**(3), 241–247.
19 X. Wu, X. Yang, R. Yu, X.-J. Zhao, Y. Zhang and W. Huang, A facile access to stiff epoxy vitrimers with excellent mechanical properties via siloxane equilibration, *J. Mater. Chem. A*, 2018, **6**(22), 10184–10188.
20 N. Wang, X. Feng, J. Pei, Q. Cui, Y. Li, H. Liu and X. Zhang, Biobased Reversible Cross-Linking Enables Self-Healing and Reprocessing of Epoxy Resins, *ACS Sustain. Chem. Eng.*, 2022, **10**(11), 3604–3613.
21 P. Wu, L. Liu and Z. Wu, A transesterification-based epoxy vitrimer synthesis enabled high crack self-healing efficiency to fibrous composites, *Composites, Part A*, 2022, **162**, 107170.
22 M. Kamble, A. Vashisth, H. Yang, S. Pranompont, C. R. Picu, D. Wang and N. Koratkar, Reversing fatigue in carbon-fiber reinforced vitrimer composites, *Carbon*, 2022, **187**, 108–114.
23 H. Memon, Y. Wei, L. Zhang, Q. Jiang and W. Liu, An imine-containing epoxy vitrimer with versatile recyclability and its application in fully recyclable carbon fiber reinforced composites, *Compos. Sci. Technol.*, 2020, **199**, 108314.
24 H. Liu, H. Zhang, H. Wang, X. Huang, G. Huang and J. Wu, Weldable, malleable and programmable epoxy vitrimers with high mechanical properties and water insensitivity, *Chem. Eng. J.*, 2019, **368**, 61–70.
25 Y. Zhang, L. Yuan, G. Liang and A. Gu, Developing Reversible Self-Healing and Malleable Epoxy Resins with High Performance and Fast Recycling through Building Cross-Linked Network with New Disulfide-Containing Hardener, *Ind. Eng. Chem. Res.*, 2018, **57**(37), 12397–12406.
26 A. A. Putnam-Neeb, J. M. Kaiser, A. M. Hubbard, D. P. Street, M. B. Dickerson, D. Nepal and L. A. Baldwin, Self-healing and polymer welding of soft and stiff epoxy thermosets via silanolates, *Adv. Compos. Hybrid Mater.*, 2022, **5**(4), 3068–3080.
27 M. Chen, L. Zhou, Y. Wu, X. Zhao and Y. Zhang, Rapid Stress Relaxation and Moderate Temperature of Malleability Enabled by the Synergy of Disulfide Metathesis and Carboxylate Transesterification in Epoxy Vitrimers, *ACS Macro Lett.*, 2019, **8**(3), 255–260.
28 F. Zhou, Z. Guo, W. Wang, X. Lei, B. Zhang, H. Zhang and Q. Zhang, Preparation of self-healing, recyclable epoxy resins and low-electrical resistance composites based on double-disulfide bond exchange, *Compos. Sci. Technol.*, 2018, **167**, 79–85.
29 P. Zheng and T. J. McCarthy, A surprise from 1954: siloxane equilibration is a simple, robust, and obvious polymer self-healing mechanism, *J. Am. Chem. Soc.*, 2012, **134**(4), 2024–2027.

30 T. Debsharma, V. Amfilochiou, A. A. Wroblewska, I. De Baere, W. Van Paepegem and F. E. Du Prez, Fast Dynamic Siloxane Exchange Mechanism for Reshapable Vitrimer Composites, *J. Am. Chem. Soc.*, 2022, **144**(27), 12280–12289.
31 T. Debsharma, S. Engelen, I. De Baere, W. Van Paepegem and F. Du Prez, Resorcinol-Derived Vitrimers and Their Flax Fiber-Reinforced Composites Based on Fast Siloxane Exchange, *Macromol. Rapid Commun.*, 2023, **44**(8), e2300020.
32 W. Xu, Y. Pan, J. Deng, L. Yin, Z. Zheng and X. Ding, Reprocessable and Self-Healing Shape Memory Epoxy Resin Based on Biphenyl Mesogen and Siloxane, *Macromol. Chem. Phys.*, 2021, **222**(23), 2100290.
33 C. Zhou, R. Li, W. Luo, Y. Chen, H. Zou, M. Liang and Y. Li, The preparation and properties study of polydimethylsiloxane-based coatings modified by epoxy resin, *J. Polym. Res.*, 2016, **23**(1), 14.
34 S. D. Al-Qahtani, R. M. Snari, K. Alkhamis, N. M. Alatawi, M. Alhasani, S. Y. Al-Nami and N. M. El-Metwaly, Development of silica-coated rare-earth doped strontium aluminate toward superhydrophobic, anti-corrosive and long-persistent photoluminescent epoxy coating, *Luminescence*, 2022, **37**(3), 479–489.
35 D. Van der Heggen, J. J. Joos, A. Feng, V. Fritz, T. Delgado, N. Gartmann, B. Walfort, D. Rytz, H. Hagemann, D. Poelman, B. Viana and P. F. Smet, Persistent Luminescence in Strontium Aluminate: A Roadmap to a Brighter Future, *Adv. Funct. Mater.*, 2022, **32**(52), 2208809.
36 J. R. N. Gnidakouong and G. J. Yun, Dislocation density level induced divergence between stress-free afterglow and mechanoluminescence in SrAl2O4: Eu2+, Dy3+, *Ceram. Int.*, 2019, **45**(2), 1794–1802.
37 Y. Fujio, C. N. Xu and N. Terasaki, Flexible Mechanoluminescent SrAl(2)O(4):Eu Film with Tracking Performance of CFRP Fracture Phenomena, *Sensors*, 2022, **22**(15), 5476.
38 A. Chairat, X. Joulia, P. Floquet, H. Vergnes, C. Ablitzer, O. Fiquet and M. Brothier, Thermal degradation kinetics of a commercial epoxy resin—comparative analysis of parameter estimation methods, *J. Appl. Polym. Sci.*, 2015, **132**(27), 42201.
39 B. K. Kandola, B. Biswas, D. Price and A. R. Horrocks, Studies on the effect of different levels of toughener and flame retardants on thermal stability of epoxy resin, *Polym. Degrad. Stab.*, 2010, **95**(2), 144–152.
40 B. Rupasinghe and J. C. Furgal, Degradation of silicone-based materials as a driving force for recyclability, *Polym. Int.*, 2021, **71**(5), 521–531.
41 W. Zhou, H. Yang, X. Guo and J. Lu, Thermal degradation behaviors of some branched and linear polysiloxanes, *Polym. Degrad. Stab.*, 2006, **91**(7), 1471–1475.
42 Y. Zhuang, X. Li, F. Lin, C. Chen, Z. Wu, H. Luo, L. Jin and R. J. Xie, Visualizing Dynamic Mechanical Actions with High Sensitivity and High Resolution by Near-Distance Mechanoluminescence Imaging, *Adv. Mater.*, 2022, **34**(36), e2202864.
43 G. H. Paulino, H. M. Yin and L. Z. Sun, Micromechanics-based Interfacial Debonding Model for Damage of Functionally Graded Materials with Particle Interactions, *Int. J. Damage Mech.*, 2016, **15**(3), 267–288.
44 A. F. Banishev and A. A. Banishev, Temperature dependence of the luminescence of powder SAOED phosphor excited by cw and pulsed laser radiation, *J. Phys.: Conf. Ser.*, 2020, **1713**, 012008.
45 L. Sharma and P. D. Sahare, Mechanoluminescence, thermoluminescence, optically stimulated luminescence and photoluminescence in SrAl(2)O(4):Eu micro- and nanophosphors: effect of particle size and annealing in different atmospheres, *RSC Adv.*, 2023, **13**(36), 25579–25598.